Masaki MIYAMOTO[1], Tetsuji MATSUO[1], Taketsune NAKAMURA[1]

Kyoto University (1)

Measurement of Vector Hysteretic Property of Silicon Steel Sheets at Liquid Nitrogen Temperature

Abstract. *This article reports vector magnetic properties of non-oriented silicon steel sheets at the liquid nitrogen temperature of 77 K. The amplitude of magnetic field decreases at 77 K under alternating and rotational flux conditions when B is large. The iron loss increases at 77 K because of the increase in eddy-current loss due to the increase in electrical conductivity.*

Streszczenie. *W artykule przedstawiono badania blachy elektrotechnicznej niezorientowanej w temperaturze ciekłego azotu 77 K. Straty mocy w tej temperaturze wzrastają na skutek wzrostu prądów wirowych spowodowanego zwiększeniem przewodności elektrycznej. (**Badanie histerezy blachy krzemowej w temperaturze ciekłego azotu**)*

Keywords: Iron loss, liquid nitrogen temperature, silicon steel, vector magnetic property.
Słowa kluczowe: blachy krzemowe, straty, ciekły azot.

Introduction

A high-temperature superconducting (HTS) induction/ synchronous motor (ISM) [1], [2] achieves high torque property efficiently over wide speed range. Its rotor and stator have usual iron-cores whose magnetic properties at very low temperature greatly affect the motor system performance.

References [3] and [4] have already reported scalar magnetic properties of silicon steel sheets at the liquid nitrogen temperature, which were measured with a compact single sheet tester (SST). However, accurate simulation of motor performance requires vector magnetic properties of silicon steel sheets.

This article reports vector magnetic properties of non-oriented silicon steel sheets at the liquid nitrogen temperature, which were measured with a compact rotational SST (RSST).

HTS Induction/Synchronous Motor

The HTS-ISM [1], [2] possesses both asynchronous and synchronous torques even though its structure is the same as the squirrel-cage-type induction motor. It is expected that the HTS-ISM realizes a gear-less and magnet-less motor system for electric vehicle achieving large torque with higher efficiency than permanent magnet motors over wide speed range.

The superconducting windings can eliminate the copper loss. Accordingly, the iron loss in the rotor and stator cores has large influence on the motor system efficiency including the refrigeration against the heat generation due to the iron loss.

Measurement at liquid nitrogen temperature

Figure 1(a) shows a stator of a conventional single-phase, two-pole induction motor that is used as a yoke of RSST [5]. Its main and auxiliary windings are used independently for two-dimensional excitation. Specifications of the induction motor are as follows: stator inner/outer diameters, 77 mm/132 mm; stator thickness, 40 mm; number of slots, 24; rated power, 200 W.

A circular sample of steel sheet with diameter of 76 mm is sandwiched between magnetic shields. The sample has 24 slits at the periphery to obtain a uniform distribution of magnetic flux density.

The RSST above is sufficiently small to be installed in a compact metal cryostat filled with liquid nitrogen. Figure 1(b) shows the RSST in the cryostat.

A two-channel function generator yields a reference vector signal for the analogue feedback system that gives sinusoidal waveforms of B_x and B_y quickly.

The cross-sectional area of steel sheets slightly reduces at the liquid nitrogen temperature of 77 K. Accordingly the area-turns of B-coils is corrected based on the thermal expansivity of steel. The area turns of H-coils are not corrected assuming that its temperature dependence is small [3], [4].

Two non-oriented silicon steel sheets (Steel A and Steel B) having the same grade (JIS: 35A300) with thickness of 0.35 mm are measured, which are provided by two different steel companies. The exciting frequencies are set at 10 and 50 Hz to separate the eddy-current loss from the hysteresis loss.

(a) (b)

Fig.1. RSST and cryostat: (a) RSST and (b) RSST installed in cryostat

Alternating Magnetic Properties

Alternating magnetic properties of Steels A and B are measured, where the amplitude of magnetic flux density, B_a, is set at 0.1, 0.2, …, 1.7 T.

Figure 2 compares the BH loops of Steel A at the liquid nitrogen temperature (77 K) and at the room temperature (RT) along the rolling direction (RD) and the transverse direction (TD) under the alternating magnetic flux condition at 50 Hz. Figure 3 depicts the BH loops of Steel B along the RD. Figures 2(c) and 3(c) show that the amplitude of H at the RT begins to sharply increase at smaller B around 1.4 T than at 77 K. This fact suggests that the transition of magnetization process to the magnetization rotation at the RT occurs with smaller B than at 77 K. A possible reason for the transition is that thermal energy fluctuation at the RT promotes the depinning of domain walls and the completion of domain-wall motion. As a result, the amplitude of H at the RT is larger than that at 77 K when B is larger than 1 T

whereas the significant amplitude change of H is not observed at small B.

The iron losses of Steels A and B per cycle are shown in Figs. 4 and 5, respectively. The loss separation is not performed at B_a = 1.6 and 1.7 T when the waveform control is not complete for large B_a at 10 Hz. Figure 6 compares the components of iron losses per cycle at B_a = 1.5 T and at 10 and 50 Hz, which are averaged values along the rolling and the transverse directions. Fig. 7 shows the ratios of hysteresis and eddy-current losses at 77 K to those at the RT. Figures 4, 5 and 6 shows that the iron loss at 77K is larger than that at the RT in spite of the decrease in the amplitude of $\boldsymbol{H}$. This is because of the increase in the eddy-current loss. Fig. 7(b) shows that the eddy-current loss of Steel A at 77K is larger by about 15 % than that at the RT. According to Ref. [3], the electrical conductivity of Steel A at 77 K is larger by 16.7 % than that at the RT, which approximately agrees with the increasing rate of eddy-current loss. This implies that the low temperature does not cause the apparent change in the anomalous eddy-current loss. The temperature has no significant influence on the hysteresis loss when $B_a \leq 1.5$ T as shown in Figs. 4, 5 and 7(a). This is related with the small temperature dependence of coercivity as is seen in Figures 2(a) and 3(a).

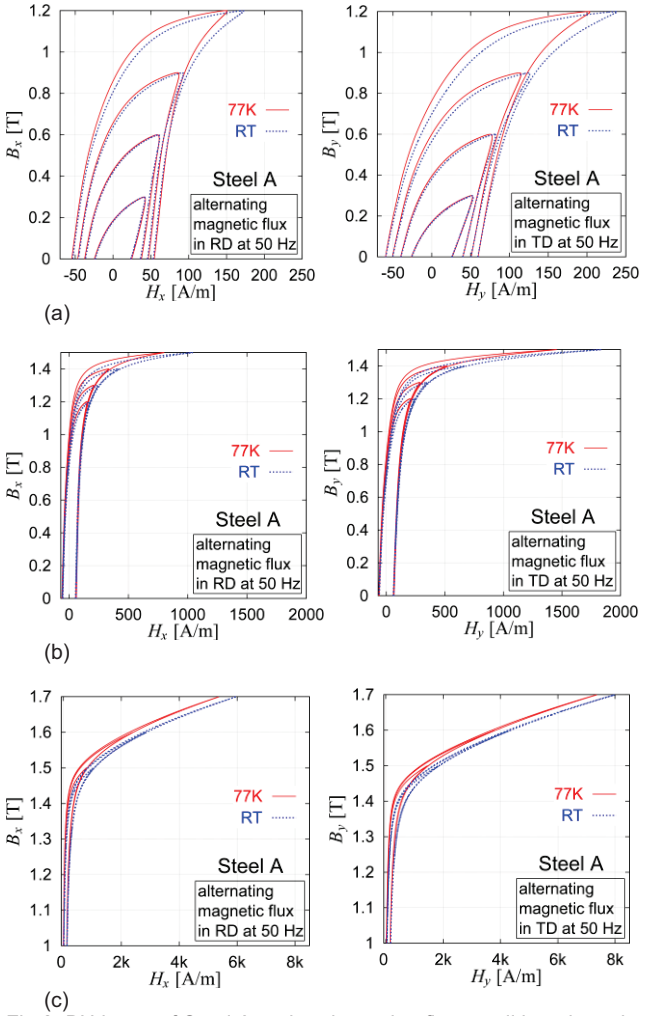

Fig.2. BH loops of Steel A under alternating flux condition along the rolling direction (left) and the transverse direction (right): (a) B_a = 0.3, 0.6, 0.9, 1.2 T, (b) B_a = 1.2, 1.3, 1.4, 1.5 T, and (c) B_a = 1.5, 1.6, 1.7 T

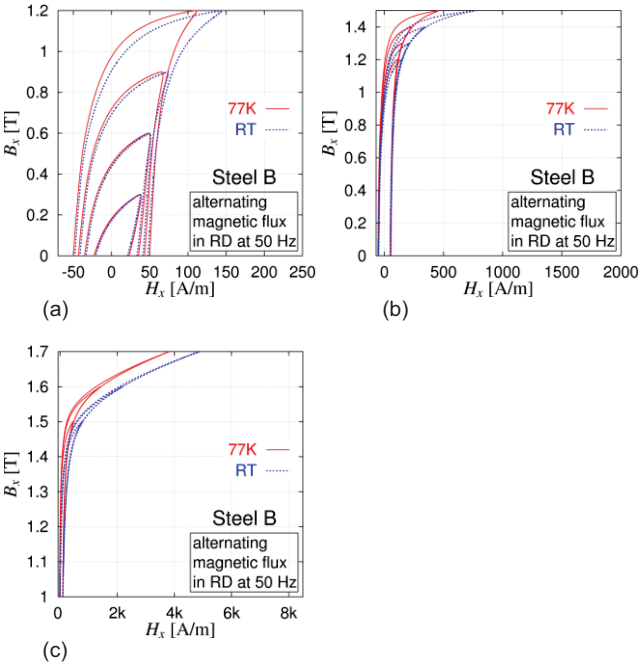

Fig.3. BH loops of Steel B under alternating flux condition along the rolling direction: (a) B_a = 0.3, 0.6, 0.9, 1.2 T, (b) B_a = 1.2, 1.3, 1.4, 1.5 T, and (c) B_a = 1.5, 1.6, 1.7 T

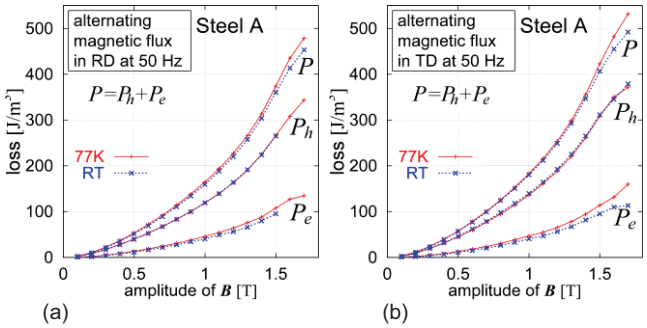

Fig.4. Iron losses of Steel A per cycle at 50 Hz under alternating flux condition where P_h, P_e and P denote the hysteresis loss, the eddy-current loss and the total iron loss, respectively: (a) along the rolling direction, and (b) along the transverse direction

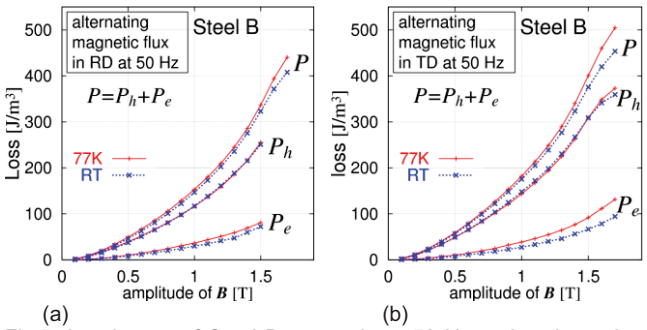

Fig.5. Iron losses of Steel B per cycle at 50 Hz under alternating flux condition where P_h, P_e and P denote the hysteresis loss, the eddy-current loss and the total iron loss, respectively: (a) along the rolling direction, and (b) along the transverse direction

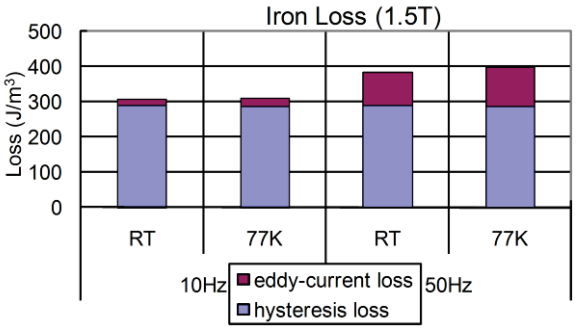

(a)

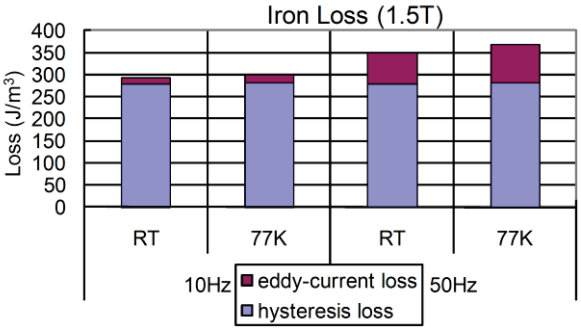

(b)

Fig.6. Iron losses per cycle at 1.5 T and at 10 and 50 Hz under alternating flux condition: (a) Steel A, and (b) Steel B

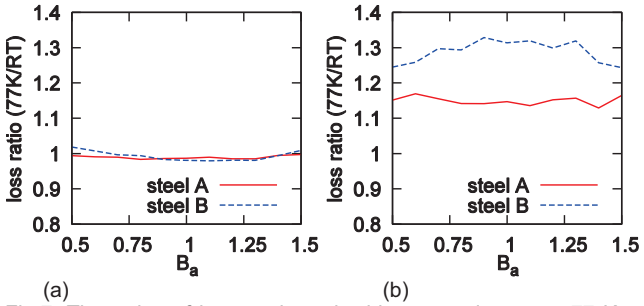

(a) (b)

Fig.7. The ratios of hysteresis and eddy-current losses at 77 K to those at the RT under alternating magnetic flux condition: (a) hysteresis loss, and (b) eddy-current loss

Rotational Magnetic Properties

Figure 8 portrays the loci of ***H*** of Steel A under the clockwise rotational magnetic flux condition at 50 Hz. When B_a is 0.4 T, the locus of ***H*** at 77 K is similar to that at the RT. When $B_a \geq 0.8$T, the amplitude of ***H*** at 77 K is smaller than that at the RT similarly to the alternating property.

The phase lag of ***B*** to ***H*** is shown in Fig. 9 under the clockwise rotational magnetic flux condition at 50 Hz. Figure 10 shows the iron loss of Steel A per cycle that is the averaged value under counter-clockwise and clockwise rotational flux conditions at 50 Hz. Figure 11 compares the components of iron losses per cycle at B_a = 1.5 T and at 10 and 50 Hz. The phase lag of ***B*** to ***H*** at 77 K is larger than that at the RT, which causes the increase in the iron loss in spite of the decrease in the amplitude of ***H***. The increase in the iron loss and phase lag is caused by the increase in the eddy-current field that is roughly proportional to the product of electrical conductivity and d***B***/d*t*. Fig. 12 shows the ratios of hysteresis and eddy-current losses at 77 K to those at the RT. The increasing ratio of eddy-current loss approximately agrees with that of electrical conductivity when B_a < 1.5 T. The temperature has no significant influence on the hysteresis loss when B_a < 1.5 T. When $B_a \geq$ 1.5 T, small increase in hysteresis loss is seen in Fig. 10.

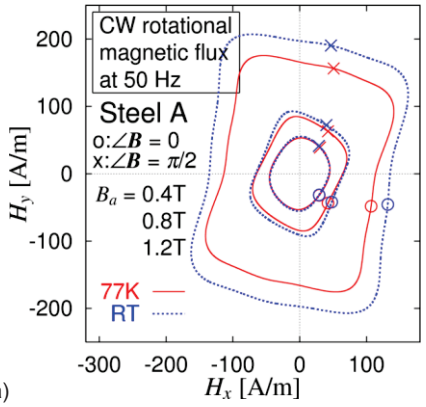

(a)

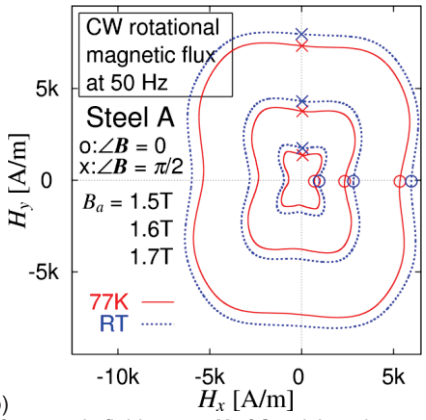

(b)

Fig.8. Loci of magnetic field vector ***H*** of Steel A under rotational flux condition, where the azimuth angle of ***B*** is 0 at "o" and it is $\pi/2$ at "x": (a) B_a = 0.4, 0.8, 1.2 ,T and (b) B_a = 1.5, 1.6, 1.7 T

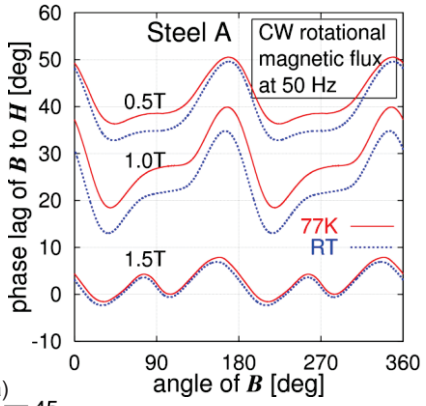

(a)

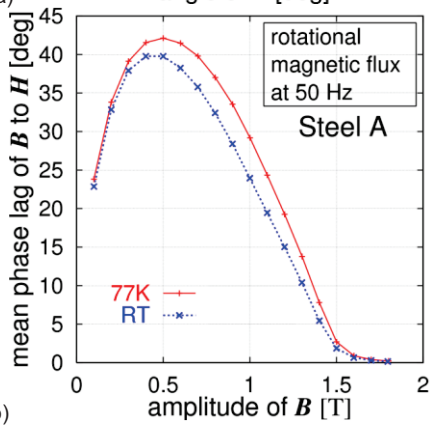

(b)

Fig.9. Phase lag of ***B*** to ***H*** of Steel A under rotational flux condition at 50 Hz: (a) dependence on azimuth angle of ***B***, and (b) dependence of averaged phase lag on amplitude of ***B***

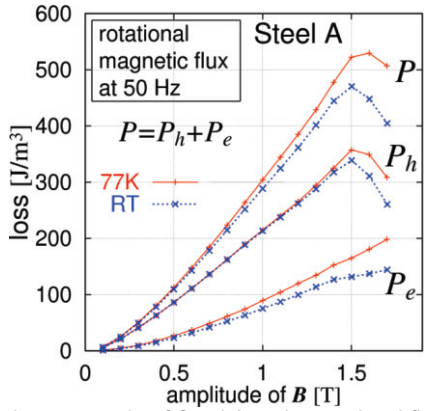

Fig.10. Iron loss per cycle of Steel A under rotational flux condition at 50 Hz

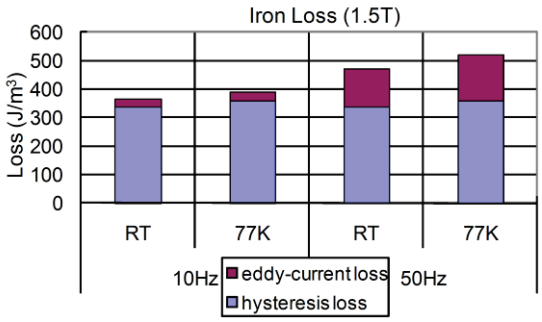

Fig.11. Iron losses per cycle of Steel A at 1.5 T and at 10 and 50 Hz under rotational flux condition

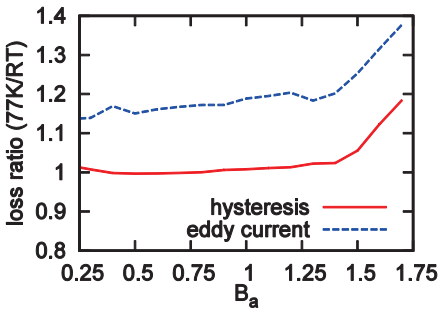

Fig.12. The ratios of hysteresis and eddy-current losses of Steel A at 77 K to those at the RT under rotational magnetic flux condition.

Fig. 12(a) shows that the increasing ratio of eddy-current loss becomes larger than that of electrical conductivity when $B_a \geq 1.5$ T. This is probably because the magnetization rotation is more dominant at the RT than at 77 K; the transition of magnetization process to the magnetization rotation reduces the rotational hysteresis loss and anomalous eddy- current loss owing to the disappearance of domain walls. However, the precise quantitative evaluation of increase in hysteresis and eddy-current loss components for large B_a is not very easy because waveforms of B_x and B_y are not completely sinusoidal when $B_a > 1.5$ T.

The iron-loss property above is similar to the scalar property reported in Refs. [3] and [4].

Conclusion

The vector magnetic properties of silicon steel sheets are measured at the liquid nitrogen temperature of 77 K. The amplitude of magnetic field decreases at 77 K under alternating and rotational flux conditions. The iron loss increases at 77 K because of the increase in the eddy-current loss due to the increase in the electrical conductivity. The temperature has no significant influence on the hysteresis loss when the amplitude of $\boldsymbol{B}$ is less than 1.5 T.

The authors express their gratitude to Prof. D. Miyagi, Tohoku University, Japan for his advice on the magnetic measurement of steel sheets at the liquid nitrogen temperature.
This work has been supported in part by the New Energy and Industrial Technology Development Organization (NEDO) in Japan.

REFERENCES

[1] Nakamura T., Ogama Y., Miyake H, K Nagao and T Nishimura, Novel rotating characteristics of a squirrel-cage-type HTS induction/ synchronous motor, *Superconductor Science & Technology*, 20(2007), no. 10, 911-918
[2] Nakamura T., Nagao K., Nishimura T. and Matsumura K., An induction/synchronous motor with high temperature superconductor/normal conductor hybrid double-cage rotor windings, *Superconductor Science & Technology*, 22(2009), no. 4, 045022
[3] Otome D., Yunoki Y., Miyagi D., Nakano M. and Takahashi N., Measurement of magnetic properties of electrical steel sheet at liquid nitrogen temperature, *Papers of Technical Meeting on Magnetics, IEE Japan*, (2008) MAG-08-78
[4] Miyagi D., Otome D., Nakano M. and Takahashi N., Measurement of magnetic properties of nonoriented electrical steel sheet at liquid nitrogen temperature using single sheet tester, IEEE Trans. Magn., 46(2010), no. 2, 314-317
[5] Matsuo T., Hirao H., and Shimasaki M., Preliminary study of 2-dimensional magnetic-property measurement of silicon steel sheet using stator of induction motor, *Przegląd Elektrotechniczny*, 83 (2007), nr 4, 67-69

***T. Matsuo**: Prof., Dept. Electrical Engineering, Graduate School of Engineering, Kyoto University, Kyoto, 615-8510 Japan, E-mail: tmatsuo@kuee.kyoto-u.ac.jp.*